CP3-Origins-2018-015 DNRF90

DO-TH 18/10

Polarized gamma rays from dark matter annihilations

Wei-Chih Huang[1,2] and Kin-Wang Ng[3,4]

[1] *CP³ Origins, University of Southern Denmark,*

Campusvej 55, DK-5230 Odense M, Denmark

[2] *Fakultät für Physik, Technische Universität Dortmund, 44221 Dortmund, Germany*

[3] *Institute of Physics, Academia Sinica, Taipei 11529, Taiwan*

[4] *Institute of Astronomy and Astrophysics,*

Academia Sinica, Taipei 11529, Taiwan

Abstract

In this paper, we explore the possibility of a linearly polarized gamma-ray signal from dark matter annihilations in the Galactic center. Considering neutral weakly interacting massive particles, a polarized gamma-ray signal can be realized by a two-component dark matter model of Majorana fermions with an anapole moment. We discuss the spin alignment of such dark matter fermions in the Galactic center and then estimate the intensity and the polarizability of the final-state electromagnetic radiation in the dark matter annihilations. For low-mass dark matter, the photon flux at sub-GeV energies may be polarized at a level detectable in current X-ray polarimeters. Depending on the mass ratio between the final-state fermion and DM, the degree of polarization at the mass threshold can reach 70% or even higher, providing us with a new tool for probing the nature of dark matter in future gamma-ray polarization experiments.

I. INTRODUCTION

Recent cosmological observations concordantly predict a spatially flat universe with 5% baryons, 25% cold dark matter (CDM), and 70% vacuum-like dark energy [1]. Unveiling the mystery of the dark components is one of the most important problems in science. Although the nature of CDM is yet unknown, it has been successfully considered as elementary weakly interacting particles (WIMPs) with regard to the relic abundance and the formation of cosmic structures. Well-motivated candidates, such as the lightest supersymmetric particle, extra dimension, hidden sector, and Higgs portal DM, have long been sought after in experimental direct and indirect searches as well as at colliders. So far all searches for WIMPs remain elusive, giving us stringent constraints on the scattering cross-sections of WIMPs with Standard Model (SM) particles (see Ref. [2] for a recent review).

In the direct-detection experiment, presumably WIMPs in the Galactic dark CDM halo scatter with target nuclei in the detector that measures the recoil energy of the nuclei, with background contamination mostly removed by the signal discrimination method. The indirect detection of WIMPs accumulated in the solar core or Galactic center (GC) is to search for signals coming from their decay or annihilation products such as gamma (γ) rays, positions, antiprotons, and neutrinos. This has been proven workable and is complementary to the direct detection; however, the observation is often masked by uncertain astrophysical background. The removal of the astrophysical background is a challenging problem, so any characteristic feature of an indirect signal will be very useful for us to distinguish between WIMPs and astrophysical background sources. Most studies of the indirect signals have concentrated on the spectral fluxes of γ rays, positions, and neutrinos, whereas the polarization of γ rays has been scarcely discussed. Since future high-energy γ-ray detectors are equipped with sensitive polarization capability [3], we aim to study the polarization of γ rays from WIMP annihilations in the GC that may enable us to separate the genuine signal from the astrophysical γ-ray background. Here we are concerned with linear polarization. The possibilities for a net circular polarization of γ rays from DM annihilations or decays have been explored in Refs. [4–8].

II. POLARIZED DM

We consider neutral WIMPs that annihilate into SM particles. In order to have polarized γ rays in the annihilation products, WIMPs must carry spins that can be aligned by an external directional field. One of possible DM models is Majorana fermions[1] with an anapole moment. In fact, such a WIMP called anapole DM has been proposed and studied [9–14] as a kind of DM that interacts with ordinary matter via a spin-current electromagnetic interaction. The interaction Hamiltonian in the non-relativistic limit is given by

$$H_I = -\frac{g}{\Lambda^2}\vec{\sigma}\cdot\vec{J}, \tag{1}$$

where g is a coupling constant, Λ is an energy scale, $\vec{\sigma}$ are the Pauli spin matrices, and $\vec{J} = \vec{\nabla}\times\vec{B}$ is the electromagnetic current density.

Observation of stellar orbits in the GC has indicated that a supermassive black hole resides at the center of the Galaxy [15]. Collective electric currents associated with gas accretion onto the black hole create large-scale magnetic fields [16]. The electric current density can be estimated as $J \sim B/h$, where B is the magnetic field strength and h is the thickness of the accretion disk. Then, the electromagnetic interaction energy (1) is of order

$$E_I \sim 10^{-29}\mathrm{eV}\, g \left(\frac{\mathrm{GeV}}{\Lambda}\right)^2 \left(\frac{B}{\mathrm{Gauss}}\right)\left(\frac{r_s}{h}\right)\left(\frac{M_\odot}{M}\right), \tag{2}$$

where M is the mass of the black hole and $r_s \equiv 2GM$ is the Schwarzschild radius. Here we use $M = 10^6 M_\odot$. The physical parameters in the accretion disk largely depend on the geometry and the temperature T of the disk [16]. For a thin and cold disk ($h \ll r_s$ and $T < 0.1\,\mathrm{keV}$), the gas energy density is typically about $1\,\mathrm{g\,cm^{-3}}$, whereas the gas is expanded to a density of about $10^{-10}\,\mathrm{g\,cm^{-3}}$ in a thick and hot disk ($h \lesssim r_s$ and $T < 0.1\,\mathrm{GeV}$). For equipartition magnetic fields, $B \sim 10^{11}\,\mathrm{Gauss}$ and $\sim 10^6\,\mathrm{Gauss}$ are in the thin-cold and the thick-hot disk, respectively. Assuming $g = 1$ and $\Lambda = 100\,\mathrm{GeV}$, the interaction energy is at least $E_I \sim 10^{-33}\mathrm{eV}$. For a thin-cold disk, $E_I \gg 10^{-28}\mathrm{eV}$.

In the presence of the directional current, the degree of spin alignment of DM particles along the current flow is governed by the Boltzmann factor, e^{-E_I/T_s}, where T_s is the spin temperature. It is difficult to determine T_s, which would depend on the history of the DM

[1] For Dirac DM, particles and antiparticles will be polarized along opposite directions and thus there is no preferred direction for DM annihilations.

halo formation and the baryonic environment. The dominant process for DM spin flips in the GC is the DM-proton scattering $D\,p \to D\,p$. Direct searches severely constrain the DM-proton cross-section $\sigma_{D\,p\to D\,p}$, which is spin-independent but velocity-suppressed in the case of anapole interactions. However, the bound becomes much less stringent for DM masses below 5 GeV or so – for 1 GeV DM, the DM-nucleon cross-section can be as large as 10^{-38} cm^2 (see, for instance, Fig. 6 in Ref. [17]) [2]. In a thick-hot disk, the proton number density in the GC is about $n_p \sim 10^{14}\,\mathrm{cm}^{-3}$ and the proton velocity is $v_p \sim 0.1c$. In the following, we assume a typical DM velocity in the DM halo, $v_D \sim 10^{-3}c$. The typical timescale for the scattering process is given by $\tau = (n_p \sigma_{D\,p\to D\,p} v)^{-1} \sim 10^8\,\mathrm{yr}$, where the relative velocity is $v \sim v_p \sim 0.1c$, which is smaller than the age of the Galaxy of order $10^{10}\,\mathrm{yr}$. As such, one would expect that the DM spins are random. However, in a thicker ($h > r_s$) and/or less hot ($T \ll 0.1\,\mathrm{GeV}$) disk, the scattering timescale may easily exceed $10^{10}\,\mathrm{yr}$. In this situation, if the initial T_s is smaller than E_I, DM will stay in the lower energy states with spins lining up with the current.

On the other hand, the thin-cold disk has $n_p \sim 10^{24}\,\mathrm{cm}^{-3}$ and $v_p \sim 10^{-4}c$. Hence we have $v \sim v_D \sim 10^{-3}c$ and that $\tau \sim 10\,\mathrm{yr}$, which is much shorter than the Galactic age. As a result of multiple DM spin flipping in the DM-proton scatterings, one would expect that DM spins are randomized and thus that $T_s \gg E_I$. However, this argument is incomplete under the consideration of the principle of minimum energy, which suggests that DM particles will relax to the ground states with spins lining up with the external current. In fact, the mechanism responsible for the energy minimization is the bremsstrahlung cooling process, $D^* p \to D\,p\,\gamma$, where $D^{(*)}$ is the ground (excited) state DM particle and γ emitted from the proton is the bremsstrahlung photon that carries away the DM kinetic energy and the excitation energy E_I. The cross-section can be estimated [19] from the DM-proton scattering process as $(\alpha/\pi)\sigma_{D\,p\to D\,p}$. The transition time for DM from the excited to ground state, that is inversely proportional to $(\alpha/\pi)\sigma_{D\,p\to D\,p} n_p v$, is $\tau \sim 10^3$ yr, which is again much shorter than the Galactic age . As long as the incoming particles have kinetic energy larger than

[2] Note that in the low-mass region, LHC searches using events with large missing transverse momentum and one or more energetic jets [18], in the context of simplified models, set limits on the cross-section: $\sigma_{D\,p\to D\,p} \lesssim 10^{-43}$ cm^2 for the vector and axial-vector interactions. The LHC bounds in general do not apply to anapole interactions as they are usually loop-induced and hence there is no resonance enhancement from the mediator as in the simplified models.

the excitation energy, the same inverse process $D\,p \to D^*p\,\gamma$ is efficient enough to reverse the spin. In the beginning, DM spins are randomized while their kinetic energy is being dissipated away by bremsstrahlung photons. During the course of the Galactic lifetime, most DM kinetic energy is lost through the bremsstrahlung cooling and subsequently a fraction of the DM is slowed down or even stopped. These slow-moving DM particles do not interact with colder gas in the outer region of the disk and eventually de-excited to the ground state by emitting virtual photons to the current background. These virtual photons are absorbed in the current by creating small perturbation in the current background of waveform, $e^{-iE_I t \pm i\vec{q}\cdot\vec{x}}$, where $\vec{q}$ is the DM momentum transfer, and the scattering amplitude is proportional to $\tilde{J}(\vec{q})$ that is the Fourier transform of the current $J(\vec{x})$. A detailed consideration of the cooling process and the de-excitation will be needed to assess the fraction of the polarized DM particles.

The above estimates, though somewhat contrived, have suggested that the anapole WIMPs may be polarized along the current flow on the accretion disk in the GC if initial DM spin temperatures are very low in some thick-hot disks. If the disk is thin and cold, a partial DM polarization may be possible. More detailed investigations should be in order, focusing on the formation of the DM halo and the accretion disk as well as the interaction between these two structures. This may help determining the DM spin temperature in the DM halo core as well as assessing the amount of DM spin alignment with the electric current in the disk.

The main interest of the present work is to propose for the first time a possibility of a linearly polarized γ-ray signal from DM annihilations. Here we have restricted ourselves to a neutral WIMP scenario, simply assuming that the WIMPs are Majorana fermions whose anapole moment allows them to be polarized in the Galactic core. Then, we consider the linear polarization of the γ rays from these DM annihilations. However, it would be interesting to explore other scenarios, for instance, by considering a dark mirror universe in which DM particles carrying dark magnetic dipole moment are polarized in an external dark magnetic field in the Galactic core. There exist many particle models for a dark mirror universe that contains dark photon; see, for instance, Refs. [20–24]. Therefore, it may not be impossible to realize in some models on what we have suggested. Overall, the capability of detecting linear polarization in future γ-ray observations will open a new window for us to look for DM and thus theoretical endeavors for a polarized γ-ray signal should be warranted.

III. PHENOMENOLOGICAL MODEL

In this phenomenological model, we have two types of Majorana DM particles χ_1 and χ_2 of the nearly equal mass m_χ. The effective Lagrangian for the anapole interaction in terms of the 4-component spinor notation reads

$$\mathcal{L} \supset \left(\frac{g}{\Lambda_1^2} \bar{\psi}_1 \gamma^\mu \gamma^5 \psi_1 + \frac{g}{\Lambda_2^2} \bar{\psi}_2 \gamma^\mu \gamma^5 \psi_2 + \frac{g}{\Lambda_3^2} \bar{\psi}_1 \left(i\gamma^\mu + A\gamma^\mu \gamma^5 \right) \psi_2 \right) \partial^\nu F_{\mu\nu} \,, \tag{3}$$

where

$$\psi_1 = \begin{pmatrix} \chi_1 \\ \chi_1^\dagger \end{pmatrix} \;,\; \psi_2 = \begin{pmatrix} \chi_2 \\ \chi_2^\dagger \end{pmatrix} \tag{4}$$

with χ_1 and χ_2 being two-component Weyl spinors[3]. Interactions such as $\bar{\chi}_i \gamma^\mu \chi_i$ do *not* exist since χ_1 and χ_2 are Majorana particles. Note that $\bar{\psi}_1 i\gamma^\mu \psi_2$ is Hermitian (real) which can be proven by the following equality:

$$\chi_i \sigma^\mu \chi_j^\dagger = -\chi_j^\dagger \bar{\sigma}^\mu \chi_i. \tag{5}$$

It is clear that χ_1 and χ_2 can be polarized along the same direction through electromagnetic anapole interactions, given a strong electric current in the GC, while the mixing term gives rise to the transition between χ_1 and χ_2, resulting in the equal amount of χ_1 and χ_2 if the transition is fast enough. Throughout this work, we assume that χ_1 and χ_2 are polarized along the same direction $\vec{S}$, denoted by the azimuthal and polar angle, ϕ and θ respectively, as shown in Fig. 1 where we set the connection between GC and the sun to be the x-axis.

Due to the facts that we intend to study γ-ray polarizations from annihilations of polarized χ_1 and χ_2 into SM fermions (f and $\bar{f}$) followed by the final state radiation as shown in Fig. 2 and that the current DM velocity is very low $v \sim 10^{-3}c$, relevant annihilation processes should be independent of the DM velocity, i.e, s-wave (total angular momentum of the DM system is zero, $L = 0$). For $\chi_{(1,2)}\chi_{(1,2)} \to \gamma \to \bar{f}f$, only one term in Eq. (3), $\bar{\psi}_1 \gamma^\mu \psi_2$, has a component of $L = 0$ with a total spin $S = 1$ [26]. By contrast, terms involving γ^5 do have a s-wave component but with $S = 0$, and so there is no preferred direction for outgoing photon polarizations in this case. All in all, we consider only the dominant process $\chi_1\chi_2 \to \bar{f}f$ induced by the operator $\bar{\psi}_1 \gamma^\mu \psi_2$. That is the reason why two Majorana DM χ_1 and χ_2 are

[3] We here follow the notations used in Ref. [25].

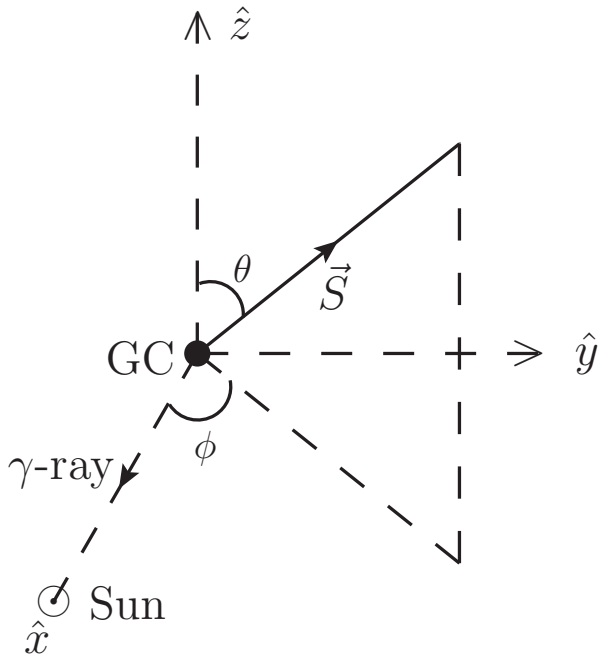

FIG. 1: The Galactic coordinate used in this work, where the sun lies on the x-axis and the DM polarization $\vec{S}$ is characterized by the polar and azimuthal angles, θ and ϕ, respectively.

required to create the polarized photon. As mentioned above, a Dirac DM candidate will not work as a particle will be polarized in an opposite direction to an antiparticle and thus there is no favored direction in particle-antiparticle annihilation.

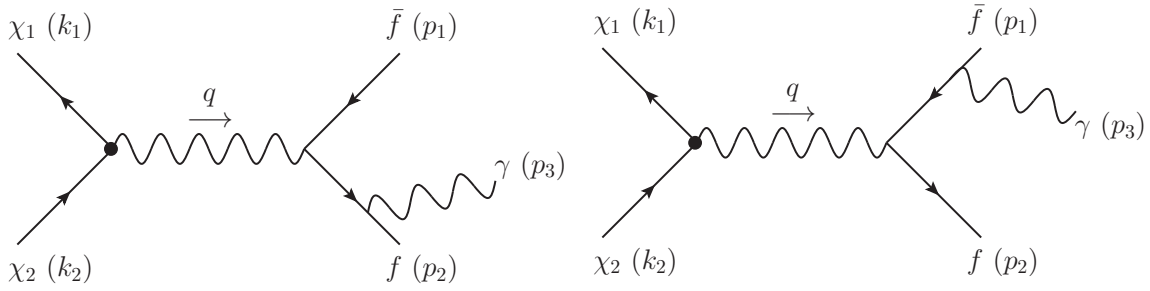

FIG. 2: Feynman diagrams for the dominant DM annihilation process $\chi_1\chi_2 \to \bar{f}f$ with final state radiation.

Employing the Feynman rules for two-component Weyl spinors [25], on the DM side the amplitude of $\chi_1 - \chi_2$ annihilation into a SM fermion pair with a prompt photon emission

is, in the limit of zero DM velocity,

$$i\mathcal{M}_1^\mu \left(\bar{\psi}_1 \gamma^\mu \psi_2\right) = \frac{ig}{\Lambda_3^2} 2m_\chi \left(0, -\cos\theta\cos\phi + i\sin\phi, -\cos\theta\sin\phi - i\cos\phi, \sin\theta\right) q^2, \tag{6}$$

where q^2, the transferred momentum squared, comes from $\partial^\nu \partial_\nu A_\mu$ and will be canceled by the denominator of the photon propagator. The other contribution from $\partial^\nu \partial_\mu A_\nu$ vanishes when contracted with $\bar{\psi}_1 \gamma^\mu \psi_2$, which can be understood by simply applying the equation of motion: $\bar{\psi}_1(k_1)(\not{k}_1 + \not{k}_2)\psi_2(k_2) \sim \bar{\psi}_1(k_1)(-m_\chi + m_\chi)\psi_2(k_2)$.

The amplitude on the SM side has two contributions corresponding to the final photon attached to either of the outgoing fermions. It is straightforward to compute the amplitude squared and sum over final fermion spins. The result reads

$$\begin{aligned}
\mathcal{M}_{2\mu}\mathcal{M}^*_{2\bar{\mu}} = Q_f^2 e^2 \Bigg(& Tr\left[\gamma_\mu \frac{\left(\not{p}_2 - \not{q} + m_f\right)}{\left(p_2 - q\right)^2 - m_f^2} \gamma_\nu \left(\not{p}_1 - m_f\right) \gamma_{\bar{\nu}} \frac{\left(\not{p}_2 - \not{q} + m_f\right)}{\left(p_2 - q\right)^2 - m_f^2} \gamma_{\bar{\mu}} \left(\not{p}_2 + m_f\right)\right] \\
& + Tr\left[\gamma_\nu \frac{\left(\not{q} - \not{p}_1 + m_f\right)}{\left(q - p_1\right)^2 - m_f^2} \gamma_\mu \left(\not{p}_1 - m_f\right) \gamma_{\bar{\mu}} \frac{\left(\not{q} - \not{p}_1 + m_f\right)}{\left(q - p_1\right)^2 - m_f^2} \gamma_{\bar{\nu}} \left(\not{p}_2 + m_f\right)\right] \\
& + \text{mixing terms} \Bigg) \epsilon^{*\nu}\left(p_3\right) \epsilon^{\bar{\nu}}\left(p_3\right),
\end{aligned} \tag{7}$$

where p_1 (p_2) is the momentum of $\bar{f}$ (f), e is the electric coupling, and Q_f is the fermion electric charge while the mixing terms refer to the interference between two diagrams in Fig. 2. The symbol ϵ^μ is the photon polarization vector; for example, $\epsilon = (0, 0, 0, 1)$ for polarization along z. Including the photon propagator, the square of the total amplitude is simply,

$$|M|^2 = \mathcal{M}_1^\mu \mathcal{M}_1^{*\bar{\mu}} \mathcal{M}_{2\mu} \mathcal{M}^*_{2\bar{\mu}} \frac{1}{\left(q^2\right)^2}, \tag{8}$$

and the corresponding differential cross-section times the DM velocity v in the limit of $v \to 0$ becomes[4]

$$v\frac{d\sigma}{d\Omega} = \frac{1}{\left(2\pi\right)^5 32 m_\chi^2} \int_{E_{3min}}^{E_{3max}} dE_3 \int_{E_{1min}}^{E_{1max}} dE_1 \int_0^{2\pi} d\gamma' |M|^2, \tag{9}$$

where γ' is the rotation angle of the final state system with respect to the photon direction and the solid angle Ω indicates that only the outgoing photons along the x-axis can reach

[4] For the 3-body phase integral, see, for instance, Ref. [2].

the earth as displayed in Fig. 1. The bounds on the energy of $\bar{f}$, given the photon energy E_3 are

$$E_{1min} = m_\chi - \frac{E_3}{2} - \frac{E_3\sqrt{m_\chi\left(m_\chi - E_3\right)\left(m_\chi^2 - m_\chi E_3 - m_f^2\right)}}{2m_\chi^2 - 2m_\chi E_3}$$
$$E_{1max} = 2m_\chi - E_3 - E_{1min}. \tag{10}$$

The minimum (maximal) E_1 occurs when the positron is along (against) the photon direction. On the other hand, the upper bound on the photon energy E_3 is

$$E_{3max} = \frac{m_\chi^2 - m_e^2}{m_\chi}, \tag{11}$$

while the minimal E_3 is determined by the detector threshold of interest[5]. As the final expression for the differential annihilation cross-section in Eq. (9) is unbearably lengthy and not very informative, we present only numerical results in the following sections.

IV. PHOTON KINEMATICAL DISTRIBUTIONS AND POLARIZATION RATE

In this section, we discuss kinematics of the photon differential distributions and the energy dependence of the polarization rate. To simplify the computation, we focus on DM annihilation in the GC where the DM density is highest and assume that the initial DM system has a total spin of one along the positive z-direction, corresponding to $\theta = \phi = 0$. It is straightforward to generalize to an arbitrary polarization direction.

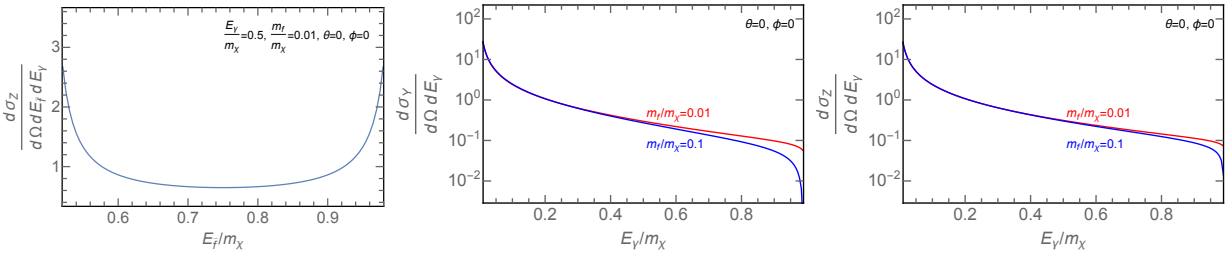

FIG. 3: Dependence of the differential annihilation cross-sections on $E_{\bar{f}}$ (left panel) and E_γ (central and right panels), assuming that the DM system is polarized along $+\hat{z}$. The subscript Z (Y) of σ refers to the z-polarized (y-polarized) photon.

[5] The cross-section in fact becomes divergent at $E_3 = 0$ and will be regulated by the virtue photon exchange. We, nonetheless, are not interested in outgoing photons with very low energies.

We start with the differential annihilation cross-section as a function of E_1 (which is $E_{\bar{f}}$) and E_3 (E_γ) displayed in Fig. 3, where the y-axis of all the panels is rescaled such that the total area below the curve is equal to unity. Given $E_\gamma/m_\chi = 0.5$ and $m_f/m_\chi = 0.01$, the left panel of Fig. 3 presents the differential cross-section for the z-polarized photons as a function of $E_{\bar{f}}$. This demonstrates that the differential cross-section are maximal when the photon is aligned with (low $E_{\bar{f}}$) or against (high $E_{\bar{f}}$) the direction of $\bar{f}$. In other words, the maximum occurs when the photon is collinear with either f or $\bar{f}$, in consistent with the statement in Ref. [19]. The same behavior exhibits in the energy spectrum of E_γ, as shown in the central panel (for y-polarized photon) and the right panel (for z-polarized photon) of Fig. 3, where $E_{\bar{f}}$ has been integrated over, and the red (blue) curve corresponds to $m_f/m_\chi = 0.01$ (0.1). The minimum of the differential cross-section occurs when both of f and $\bar{f}$ are in the same direction but opposite to that of the photon.

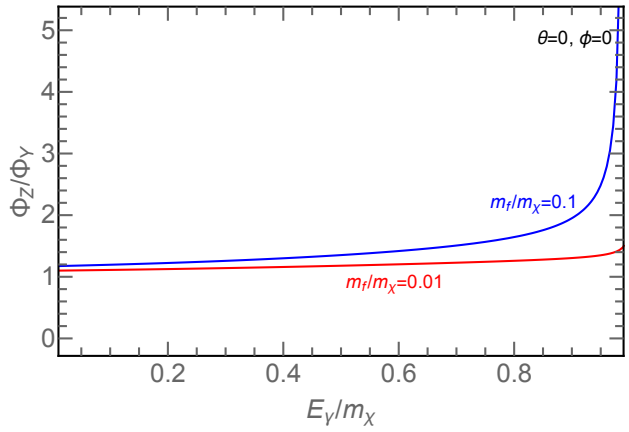

FIG. 4: The flux ratio of the z-polarized to y-polarized photon as a function of E_γ, assuming both χ_1 and χ_2 be polarized along $+\hat{z}$.

Fig. 4 shows the ratio of the differential cross-section of the z-polarized photon to that of the y-polarized one as a function of E_γ, assuming that the DM particles $\chi_{1,2}$ are polarized along the positive z-direction. This ratio is equivalent to the ratio of the corresponding photon fluxes Φ_Z/Φ_Y. We present two cases of different mass ratios: $m_f/m_\chi = 0.1$ (blue line) and $m_f/m_\chi = 0.01$ (red line). It is clear that outgoing photons are more likely to have the polarization along the z- than y-direction.

In general, the photons with larger energies are more likely to be polarized along the z-direction than those with smaller energies. It can be understood in a naive argument based

on angular momentum conservation as follows. First, the electric current couples a left-handed particle to a right-handed anti-particle (or a right-handed particle to a left-handed anti-particle). Second, in the massless limit, the fermion chirality coincides with the helicity, which is the projection of the spin onto the direction of momentum. Third, for the high-

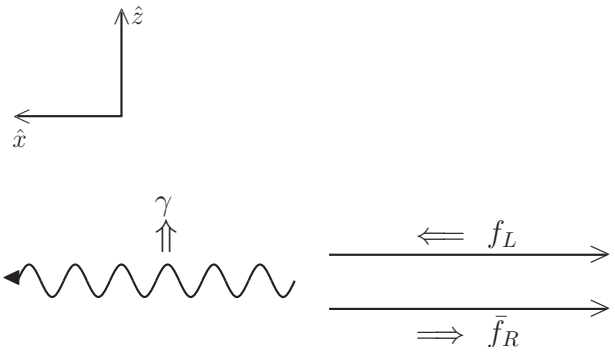

FIG. 5: The pictorial explanation of why Φ_Z/Φ_Y increases as E_γ becomes larger. For the energetic photon, the spins of the pair fermions cancel out so that the photon is polarized along the same direction as the total angular momentum of the initial DM system, i.e., $+\hat{z}$.

energy photon with f and $\bar{f}$ moving in the same direction, the spin angular momenta of f and $\bar{f}$ cancel each other such that the polarization of the photon has to be in the z-direction to conserve the angular momentum as displayed in Fig. 5, given that the initial DM system has $\vec{L} = 0$ and $\vec{S} = +\hat{z}$. Consequently, the high-energy photons tend to be polarized along the z-direction. By contrast, for the low energy photon, the spins of the fermion pair add up to unity along the x-direction. In this case, a nonzero orbital angular momentum of the final states is required to conserve the total angular momentum, rendering Φ_Z/Φ_Y smaller.

On the other hand, it is noticeable that with a larger value of m_f/m_χ the photon polarization becomes more pronounced. For the low-energy photons, it can be explained by a chirality flip due to the existence of the mass term as displayed in Fig. 6. To be more concrete, because of the mass term, there exists a finite possibility that even the right-handed $\bar{f}$ can have a left-handed helicity – heavier mass, higher probability – so that the spins of the fermion pair cancel each other, leading to the z-polarized photon. On the other hand, for the high-energy region, with larger m_f/m_χ the Φ_Y decreases more dramatically than Φ_Z as the energy increases. This can be seen by comparing the blue lines between the central and right panels of Fig. 3. As a result, Φ_Z/Φ_Y becomes much larger for E_γ/m_χ close to unity.

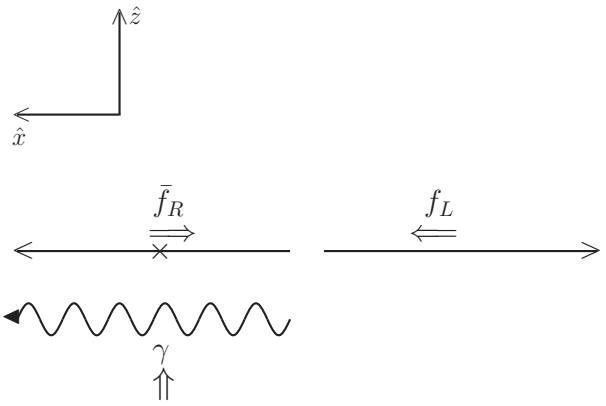

FIG. 6: The pictorial explanation of how a chirality flip (a mass insertion) can increase the possibility of having the z-polarization for the low-energy photons.

V. ESTIMATION OF POLARIZED PHOTON FLUX

As explained above, the only annihilation process with nonzero spin is induced by the operator $\bar{\chi_1}\gamma^\mu\chi_2\partial^\nu F_{\mu\nu}$, which can be rewritten as $\bar{\chi_1}\gamma^\mu\chi_2\bar{f}\gamma_\mu f$. The expected photon flux on Earth from DM annihilation $\chi_1\chi_2 \to \bar{f}f$ at the GC followed by final state radiation (see Fig. 2) is [6]

$$\frac{d\Phi}{d\Omega dE_\gamma} = \frac{r_\odot}{4}\left(\frac{\rho_\odot}{m_\chi}\right)^2 J \sum_f \frac{d\sigma(\chi_1\chi_2 \to \bar{f}f\gamma)}{d\Omega dE_\gamma} v\,, \tag{12}$$

where $\rho_\odot = 0.3$ GeV/cm^3, $r_\odot = 8.33$ kpc, and v is the relative velocity between χ_1 and χ_2, while J stands for the J factor, corresponding to the DM density (squared) integral along the line of sight given a solid angle $d\Omega$:

$$J = \int_{\text{l.o.s}} \frac{ds}{r_\odot}\left(\frac{\rho}{\rho_\odot}\right)^2 . \tag{13}$$

Here, we assume χ_1 and χ_2 have the same density and be polarized along $+\hat{z}$. This results in an anisotropic system. Then, instead of the conventional assumption of the isotropic photon distribution that leads to a factor of 4π in the denominator, $d\sigma/d\Omega dE_\gamma$ is employed in Eq. (12) and can be computed based on Eq. (9).

On the other hand, the same operator will also give rise to sizable spin-independent

[6] For DM-induced photon flux computations, see, e.g., Ref. [28] for more details.

DM-proton interactions $\chi_{(1,2)}p \to \chi_{(2,1)}p$,

$$\sigma_{\text{DM-p}} = \frac{e^4\mu^2}{\pi\Lambda_3^4}\,, \tag{14}$$

where μ is the reduced mass of the DM-proton system and the coupling constant g in Eq. (3) is set to the electric coupling e. For m_χ below 5 GeV or so, the bounds on the spin-independent DM-nucleon cross-section become much weaker, implying a smaller Λ_3 and hence a larger photon flux from $\chi_1 - \chi_2$ annihilation. In Fig. 7, we show the expected γ-ray flux for 1 GeV (blue solid line) and 4 GeV (red solid line, which is the flux multiplied by a factor of 100), while the purple dashed line represents the GC γ-ray excess taken from Ref. [29] for the region of interest, $|\ell| \leq 20^\circ$ and $2^\circ \leq |b| \leq 20^\circ$, which has $J = 25.8$, assuming the Navarro-Frenk-White (NFW) DM profile [30]. The entries in the parentheses

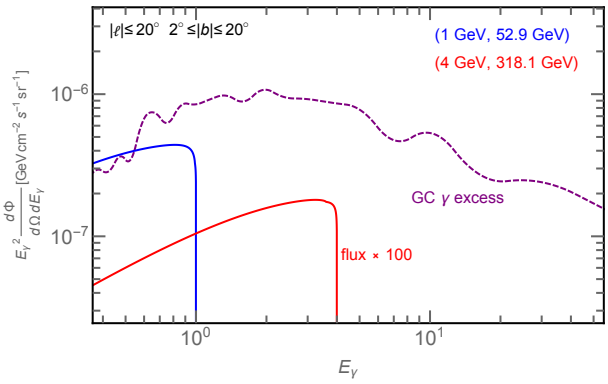

FIG. 7: γ flux from DM annihilation

indicate the values of m_χ and Λ_3 respectively, where $\sigma^{\text{SI}}_{\text{DM-nucleon}} \leq 9 \times 10^{-39}$ (1.7×10^{-41}) cm^2 for DM of 1 (4) GeV from the CRESST-II [31] (CDMSlite [32]) experiment are used. Clearly, DM of 4 GeV is more constrained by direct detection than 1 GeV DM, resulting in a larger value of Λ_3 and thus a smaller photon flux. For 1 GeV DM, the photon flux is comparable to the GC γ-ray excess. Note that the values of Λ_3 assumed here actually lead to a smaller DM annihilation cross-section than required, i.e., one will end up with a too large DM relic density. This issue can be solved by including Λ_1 and Λ_2 terms in Eq. (3) to increase the DM annihilation rate during freeze-out, but the polarization rate will be reduced as the γ_5 terms have $\vec{L} = \vec{S} = 0$ contributions.

To conclude, the possibility of detecting polarized photons will depend on how many of DM particles at the GC are polarized and also depend on the DM mass. For a light

DM below 5 GeV, a preferred direction for the photon polarization could potentially be detectable if a significant part of the DM particles is polarized along a certain direction around the GC. For heavier DM, the photon flux is hopelessly small because of the stringent direct search bounds.

VI. CONCLUSIONS AND OUTLOOK

The azimuthal angle of the plane of production of an electron-positron pair created in a γ-ray detector provides a way of measuring linear polarization of incoming γ rays. The current γ-ray detectors are not designed primarily for polarization measurement. Instruments sensitive to linear polarization will be employed in future γ-ray experiments such as AdEPT and ASTROGAM, with the minimum detectable polarization (MDP) from a few percents up to 20% or so [33].

In this work, we have proposed a simple phenomenological model where two types of Majorana DM particles, degenerate in mass, have anapole interactions. The anapole interactions can polarize the spins of DM in the presence of electric currents at the GC, and in turn the linearly polarized γ-ray flux from DM annihilations can be realized. The degree of polarization of the γ rays can reach as much as 70% at the DM mass threshold, given the mass ratio of the final state fermion to DM being 0.1. For a larger mass ratio, a higher polarization rate is expected. For DM mass of about 1 GeV, the γ-ray flux can be comparable to the γ-ray excess in the GC. The origin of the GC excess is still a puzzle, probably comprised of diffuse γ rays from multiple components of many different sources and thus being most likely unpolarized. Therefore, any detection of polarized γ rays may give an invaluable understanding of the GC excess. Even though the DM induced γ-ray flux is an order of magnitude below the GC excess, the polarization measurement can still be used to identify a highly polarized γ-ray signal. In addition, the photon flux induced by GeV DM has a plateau shape extending to sub-GeV energies, though the degree of polarization drops to $\lesssim 10\%$. This polarized low-energy γ-ray signal may be of interest to current X-ray telescopes such as the POLAR satellite, which is a X-ray polarimeter sensitive to an energy up to 0.5 MeV with a 10% MDP [34].

As we have explained how the spins of anapole DM can be aligned with the electric current flow in the GC, unfortunately it is rather difficult to determine the degree of alignment

without knowing the details of the formation of the dark halo and the accretion disk. A low degree of alignment will definitely degrade the detectability of a polarized signal. Here we stress that the present paper has given a first attempt to investigate a possible *linearly* polarized γ-ray signal from DM annihilations. It is certainly important to explore further along this direction for making full use of the polarization capability of future γ-ray detectors.

Acknowledgments

WCH is grateful for the hospitality of IOP Academia Sinica and NCTS in Taiwan, where this work was initiated. WCH was supported by DGF Grant No. PA 803/10-1 and by the Independent Research Fund Denmark, grant number DFF 6108-00623. KWN is supported by Ministry of Science and Technology, Taiwan, ROC under the Grant No. MOST104-2112-M-001-039-MY3. The CP3-Origins centre is partially funded by the Danish National Research Foundation, grant number DNRF90.

[1] P. A. R. Ade et al. Planck 2015 results. XIII. Cosmological parameters. *Astron. Astrophys.*, 594:A13, 2016, 1502.01589.

[2] K. A. Olive. Review of Particle Physics. *Chin. Phys.*, C40(10):100001, 2016.

[3] Felix A. Aharonian, Werner Hofmann, and Frank M. Rieger, editors. *Proceedings, 6th International Symposium on High-Energy Gamma-Ray Astronomy (Gamma 2016)*, volume 1792, 2017.

[4] Alejandro Ibarra, Sergio Lopez-Gehler, Emiliano Molinaro, and Miguel Pato. Gamma-ray triangles: a possible signature of asymmetric dark matter in indirect searches. *Phys. Rev.*, D94(10):103003, 2016, 1604.01899.

[5] Jason Kumar, Pearl Sandick, Fei Teng, and Takahiro Yamamoto. Gamma-ray Signals from Dark Matter Annihilation Via Charged Mediators. *Phys. Rev.*, D94(1):015022, 2016, 1605.03224.

[6] W. Bonivento, D. Gorbunov, M. Shaposhnikov, and A. Tokareva. Polarization of photons emitted by decaying dark matter. *Phys. Lett.*, B765:127–131, 2017, 1610.04532.

[7] Céline Bœhm, Céline Degrande, Olivier Mattelaer, and Aaron C. Vincent. Circular polarisation: a new probe of dark matter and neutrinos in the sky. *JCAP*, 1705(05):043, 2017, 1701.02754.

[8] Andrey Elagin, Jason Kumar, Pearl Sandick, and Fei Teng. On the Prospects for Detecting a Net Photon Circular Polarization Produced by Decaying Dark Matter. 2017, 1709.03058.

[9] Maxim Pospelov and Tonnis ter Veldhuis. Direct and indirect limits on the electromagnetic form-factors of WIMPs. *Phys. Lett.*, B480:181–186, 2000, hep-ph/0003010.

[10] Chiu Man Ho and Robert J. Scherrer. Anapole Dark Matter. *Phys. Lett.*, B722:341–346, 2013, 1211.0503.

[11] A. Liam Fitzpatrick and Kathryn M. Zurek. Dark Moments and the DAMA-CoGeNT Puzzle. *Phys. Rev.*, D82:075004, 2010, 1007.5325.

[12] Mads T. Frandsen, Felix Kahlhoefer, Christopher McCabe, Subir Sarkar, and Kai Schmidt-Hoberg. The unbearable lightness of being: CDMS versus XENON. *JCAP*, 1307:023, 2013, 1304.6066.

[13] Moira I. Gresham and Kathryn M. Zurek. Light Dark Matter Anomalies After LUX. *Phys.*

Rev., D89(1):016017, 2014, 1311.2082.

[14] Eugenio Del Nobile, Graciela B. Gelmini, Paolo Gondolo, and Ji-Haeng Huh. Direct detection of Light Anapole and Magnetic Dipole DM. *JCAP*, 1406:002, 2014, 1401.4508.

[15] S. Gillessen, F. Eisenhauer, S. Trippe, T. Alexander, R. Genzel, F. Martins, and T. Ott. Monitoring stellar orbits around the Massive Black Hole in the Galactic Center. *Astrophys. J.*, 692:1075–1109, 2009, 0810.4674.

[16] S. L. Shapiro and S. A. Teukolsky. *Black holes, white dwarfs, and neutron stars: The physics of compact objects*. New York, USA: Wiley 645 p, 1983.

[17] F. Petricca et al. First results on low-mass dark matter from the CRESST-III experiment. In *15th International Conference on Topics in Astroparticle and Underground Physics (TAUP 2017) Sudbury, Ontario, Canada, July 24-28, 2017*, 1711.07692.

[18] Search for dark matter in final states with an energetic jet, or a hadronically decaying W or Z boson using 12.9 fb^{-1} of data at $\sqrt{s} = 13$ TeV. *CMS-PAS-EXO-16-037*, 2016.

[19] Andreas Birkedal, Konstantin T. Matchev, Maxim Perelstein, and Andrew Spray. Robust gamma ray signature of WIMP dark matter. 2005, hep-ph/0507194.

[20] Robert Foot, H. Lew, and R. R. Volkas. A Model with fundamental improper space-time symmetries. *Phys. Lett.*, B272:67–70, 1991.

[21] Z. G. Berezhiani, A. D. Dolgov, and R. N. Mohapatra. Asymmetric inflationary reheating and the nature of mirror universe. *Phys. Lett.*, B375:26–36, 1996, hep-ph/9511221.

[22] Zurab Berezhiani, Denis Comelli, and Francesco L. Villante. The early mirror universe: Inflation, baryogenesis, nucleosynthesis and dark matter. *Phys. Lett.*, B503:362–375, 2001, hep-ph/0008105.

[23] Z. Chacko, Hock-Seng Goh, and Roni Harnik. The Twin Higgs: Natural electroweak breaking from mirror symmetry. *Phys. Rev. Lett.*, 96:231802, 2006, hep-ph/0506256.

[24] Wei-Chih Huang, Yue-Lin Sming Tsai, and Tzu-Chiang Yuan. G2HDM : Gauged Two Higgs Doublet Model. *JHEP*, 04:019, 2016, 1512.00229.

[25] Herbi K. Dreiner, Howard E. Haber, and Stephen P. Martin. Two-component spinor techniques and Feynman rules for quantum field theory and supersymmetry. *Phys. Rept.*, 494:1–196, 2010, 0812.1594.

[26] Jason Kumar and Danny Marfatia. Matrix element analyses of dark matter scattering and annihilation. *Phys. Rev.*, D88(1):014035, 2013, 1305.1611.

[27] Wei-Chih Huang, Alfredo Urbano, and Wei Xue. Fermi Bubbles under Dark Matter Scrutiny Part II: Particle Physics Analysis. *JCAP*, 1404:020, 2014, 1310.7609.

[28] Marco Cirelli, Gennaro Corcella, Andi Hektor, Gert Hutsi, Mario Kadastik, Paolo Panci, Martti Raidal, Filippo Sala, and Alessandro Strumia. PPPC 4 DM ID: A Poor Particle Physicist Cookbook for Dark Matter Indirect Detection. *JCAP*, 1103:051, 2011, 1012.4515. [Erratum: JCAP1210,E01(2012)].

[29] Francesca Calore, Ilias Cholis, and Christoph Weniger. Background Model Systematics for the Fermi GeV Excess. *JCAP*, 1503:038, 2015, 1409.0042.

[30] Julio F. Navarro, Carlos S. Frenk, and Simon D. M. White. The Structure of Cold Dark Matter Halos. *Astrophys. J.*, 462:563–575, 1996, astro-ph/9508025.

[31] G. Angloher et al. Results on light dark matter particles with a low-threshold CRESST-II detector. *Eur. Phys. J.*, C76(1):25, 2016, 1509.01515.

[32] R. Agnese et al. New Results from the Search for Low-Mass Weakly Interacting Massive Particles with the CDMS Low Ionization Threshold Experiment. *Phys. Rev. Lett.*, 116(7):071301, 2016, 1509.02448.

[33] Jürgen Knödlseder. The future of gamma-ray astronomy. *Comptes Rendus Physique*, 17:663–678, 2016, 1602.02728.

[34] Merlin Kole. Polarimetry with POLAR. *PoS*, MULTIF2017:068, 2018, 1804.04864.